

Batch simulations and uncertainty quantification in Gaussian process surrogate ABC

1 BACKGROUND ON ABC INFERENCE

- **Approximate Bayesian computation (ABC)** is used for Bayesian inference when the likelihood function $\pi(\mathbf{x}|\theta)$ is intractable but simulating pseudo-data $\mathbf{x} \in \mathcal{X}$ is feasible.
- The intractable posterior $\pi(\theta|\mathbf{x}_0)$ is approximated with

$$\pi_{\text{ABC}}(\theta|\mathbf{x}_0) \triangleq \frac{\pi(\theta) \int_{\mathcal{X}} \pi_{\varepsilon}(\mathbf{x}_0|\mathbf{x}) \pi(\mathbf{x}|\theta) d\mathbf{x}}{\int_{\Theta} \pi(\theta') \int_{\mathcal{X}} \pi_{\varepsilon}(\mathbf{x}_0|\mathbf{x}') \pi(\mathbf{x}'|\theta') d\mathbf{x}' d\theta'}, \quad (1)$$

where $\pi_{\varepsilon}(\mathbf{x}_0|\mathbf{x}) = \mathbb{1}_{\Delta(\mathbf{x}_0, \mathbf{x}) \leq \varepsilon}$, $\Delta: \mathcal{X}^2 \rightarrow \mathbb{R}_+$ is a discrepancy function and ε is a threshold parameter.

- Common sampling-based ABC methods targeting (1) require huge number of simulations and cannot be used when **simulations are costly**.
- Recently various approaches using neural networks and Gaussian process (GP) **surrogate models** have been proposed to tackle the computational challenges.

2 CONTRIBUTIONS

- Reformulation of earlier GP-surrogate based approaches [1, 2, 3] into a coherent framework called '**Bayesian ABC**'.
- **Batch Bayesian experimental design (active learning)** strategies for the parallelisation of the potentially expensive simulations in this framework.
- An approach to **quantify the uncertainty** in the moments and marginals of the ABC posterior.
- Further analysis on the connections between the related problems of **Bayesian ABC**, **Bayesian quadrature** and **Bayesian optimisation**.
- Extensive experiments with several toy and real-world simulation models with intractable likelihoods.

3 BAYESIAN ABC FRAMEWORK

- **Bayesian ABC** uses another layer of Bayesian inference to estimate the ABC posterior in (1). The previously simulated discrepancy-parameter-pairs $D_t = \{(\Delta_i, \theta_i)\}_{i=1}^t$ are treated as 'data' to learn a **GP surrogate model**, which will predict the discrepancy for a given parameter value. The GP model is used to form an estimator for the ABC posterior (1) and to **adaptively acquire new data**.
- Each discrepancy evaluation Δ_i at corresponding parameter θ_i is assumed to be generated as

$$\Delta_i = f(\theta_i) + \nu_i, \quad \nu_i \stackrel{\text{i.i.d.}}{\sim} \mathcal{N}(0, \sigma_n^2), \quad (2)$$

where $\sigma_n^2 > 0$ is the variance of the discrepancy.

- To encode the assumptions of e.g. smoothness and quadratic shape of Δ_{θ} , f is given a GP prior.
- If f and σ_n^2 were known, the ABC posterior could be obtained from (1) and (2) as

$$\pi_{\text{ABC}}^f(\theta) \triangleq \frac{\pi(\theta) \Phi((\varepsilon - f(\theta))/\sigma_n)}{\int_{\Theta} \pi(\theta') \Phi((\varepsilon - f(\theta'))/\sigma_n) d\theta'}, \quad (3)$$

- Computing the distribution of π_{ABC}^f is difficult due to its non-linear dependence on infinite-dimensional quantity f . However, various statistics of $\pi_{\text{ABC}}^f(\theta) \triangleq \pi(\theta) \Phi((\varepsilon - f(\theta))/\sigma_n)$, the numerator of (3), can be computed analytically [2] and combined with MCMC.
- Given D_t , our knowledge about f is $f \sim \Pi_{D_t}^f \triangleq \mathcal{GP}(f; m_t, c_t)$. The posterior of π_{ABC}^f in (3) describes the amount of uncertainty in π_{ABC}^f due to the limited t simulations and is obtained as the push-forward measure through the mapping $f \mapsto \pi_{\text{ABC}}^f$.
- We developed a numerical method to characterise this uncertainty based on normalised importance sampling and GP sample paths. For illustration, see Fig. 1c-d and 5.

Bayesian ABC vs. Bayesian quadrature vs. Bayesian optimisation

- **Bayesian ABC**: 'estimate' π_{ABC}^f in (3) (or π_{ABC}^f). Data: $D_t = \{(\Delta_i, \theta_i)\}_{i=1}^t$. Model: $\Delta_i \sim \mathcal{N}(f(\theta_i), \sigma_n^2)$, $f \sim \mathcal{GP}$, typically $\sigma_n \gg 0$.
- **Bayesian quadrature**: 'estimate' $I \triangleq \int g[f(\theta)] \pi(\theta) d\theta$ where usually $g[f(\theta)] = f(\theta)$. Data: $\{(\nu_i, \theta_i)\}_{i=1}^t$. Model: $y_i \sim \mathcal{N}(f(\theta_i), \sigma_n^2)$, $f \sim \mathcal{GP}$, typically $\sigma_n \approx 0$.
- **BayesOpt**: 'estimate' $\theta^* \triangleq \arg \min_{\theta} f(\theta)$. Data: $\{(\nu_i, \theta_i)\}_{i=1}^t$. Model: $y_i \sim \mathcal{N}(f(\theta_i), \sigma_n^2)$, $f \sim \mathcal{GP}$, typically $\sigma_n \approx 0$.

REFERENCES

- [1] M. U. Gutmann and J. Corander. Bayesian optimization for likelihood-free inference of simulator-based statistical models. *Journal of Machine Learning Research*, 17(125):1–47, 2016.
- [2] M. Järvenpää, M. U. Gutmann, A. Pleska, A. Vehtari, and P. Marttinen. Efficient acquisition rules for model-based approximate Bayesian computation. *Bayesian Analysis*, 14(2):595–622, 2019.
- [3] M. Järvenpää, M. U. Gutmann, A. Vehtari, and P. Marttinen. Parallel Gaussian process surrogate Bayesian inference with noisy likelihood evaluations. *Bayesian analysis*, to appear, 2020.
- [4] O. Thomas, R. Dutta, J. Corander, S. Kaski, and M. U. Gutmann. Likelihood-free inference by ratio estimation. *arXiv1611.10242*, 2018.
- [5] E. Numminen, L. Cheng, M. Gyllenberg, and J. Corander. Estimating the transmission dynamics of streptococcus pneumoniae from strain prevalence data. *Biometrics*, 69(3):748–757, 2013.

4 BATCH ACQUISITION FUNCTIONS

- Need to find **informative simulation locations** for estimating π_{ABC}^f in (3) given the postulated GP model.
- Loss function $l(\pi_{\text{ABC}}, d)$ quantifies the penalty of reporting $d \in \mathcal{D}$ as our ABC posterior when the true one is $\pi_{\text{ABC}} \in \mathcal{D}$. Given D_t , the one-batch-ahead **Bayes-optimal** selection of the **next batch** $\theta^{\text{opt}} = [\theta_1^{\text{opt}}, \dots, \theta_b^{\text{opt}}]$ is $\theta^{\text{opt}} = \arg \min_{\theta^* \in \Theta^b} L_t(\theta^*)$, where

$$L_t(\theta^*) = \mathbb{E}_{\Delta^* | \theta^*, D_t} \min_{d \in \mathcal{D}} \mathbb{E}_f | D_t \cup D^* l(\pi_{\text{ABC}}^f, d). \quad (4)$$

- If we use L^2 loss function $\tilde{l}_2 \triangleq \int_{\Theta} (\pi_{\text{ABC}}^f(\theta) - \tilde{d}(\theta))^2 d\theta$, then the optimal estimator for π_{ABC}^f is the mean and the resulting **expected integrated variance (EIV) acquisition function**, denoted as $L_t^{\text{EIV}}(\theta^*)$, is

$$L_t^{\text{EIV}}(\theta^*) = 2 \int_{\Theta} \pi^2(\theta) \left[T \left(a_t(\theta), \frac{\sqrt{\sigma_n^2 + s_t^2(\theta) - \tau_t^2(\theta; \theta^*)}}{\sqrt{\sigma_n^2 + s_t^2(\theta) + \tau_t^2(\theta; \theta^*)}} \right) - T \left(a_t(\theta), \sigma_n / \sqrt{\sigma_n^2 + 2s_t^2(\theta)} \right) \right] d\theta, \quad (5)$$

where $a_t(\theta) \triangleq (\varepsilon - m_t(\theta)) / \sqrt{\sigma_n^2 + s_t^2(\theta)}$, $s_t^2(\theta) = c_t(\theta, \theta)$, $\tau_t^2(\theta; \theta^*) = c_t(\theta, \theta^*) [c_t(\theta^*, \theta^*) + \sigma_n^2]^{-1} c_t(\theta^*, \theta)$ and T is Owen's T function.

- Similarly, L^1 loss function produces the marginal median as the optimal estimator for π_{ABC}^f and results **expected integrated MAD (EIMAD) acquisition function**.
- We use **greedy optimisation** and the integral over Θ is approximated using **importance sampling**.
- Heuristically-motivated batch methods (MAXV, MAXMAD) based on **uncertainty sampling** and random strategy RAND are used as baselines.

Illustration of the main idea

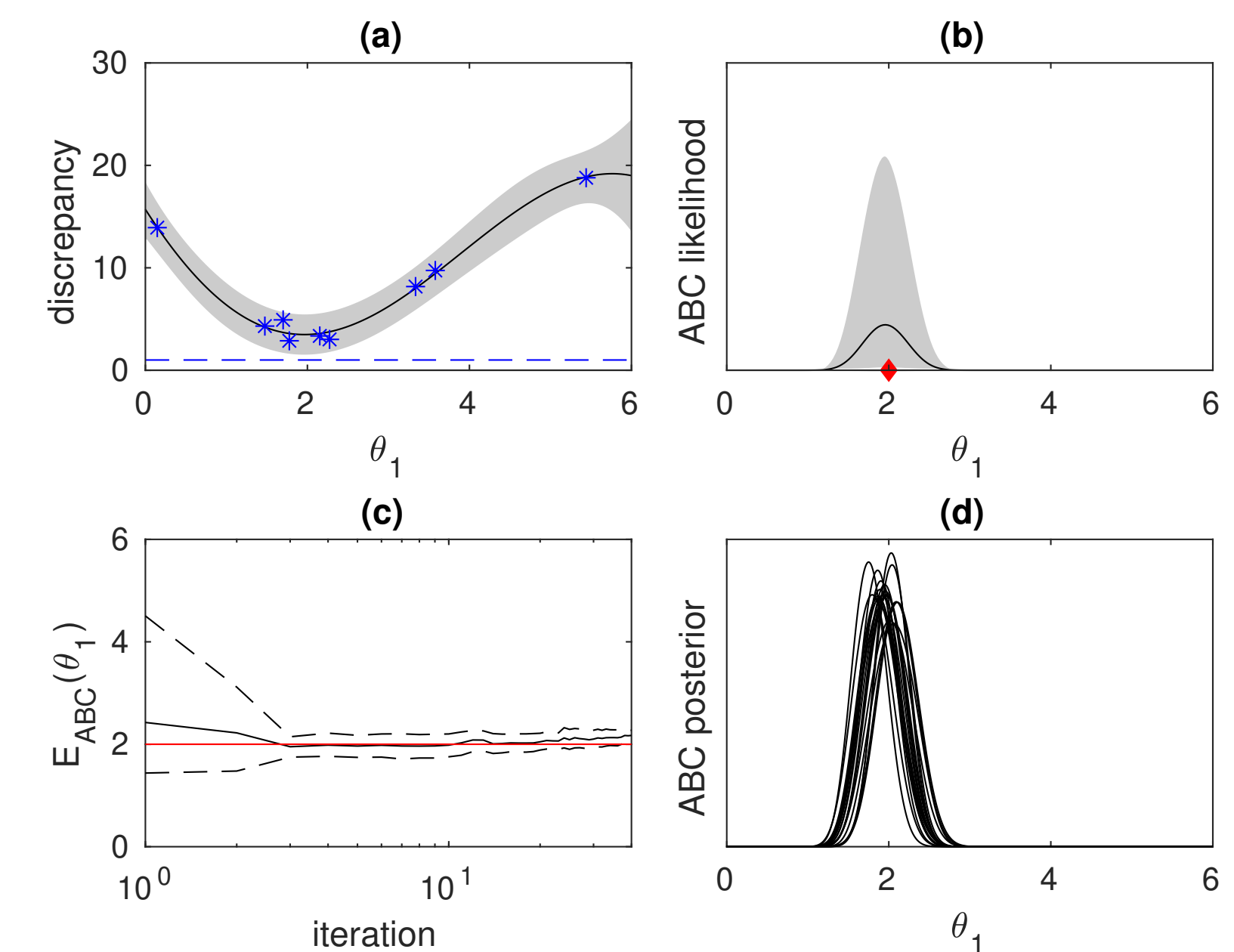


Figure 1: ABC posterior uncertainty quantification using Lorenz model with parameter θ_2 fixed. (a) GP for Δ_{θ_1} (blue dashed line ε , blue stars 9 discrepancy evaluations), (b) uncertainty of unnormalised ABC posterior π_{ABC}^f , (c) evolution of GP-based ABC posterior expectation (black line) and its 95% CI (dashed black) for 40 iterations, (d) uncertainty of ABC posterior π_{ABC}^f .

5 MAIN RESULTS

- Experiments show that ABC posterior uncertainty quantification approach is useful in low dimensions and that **Bayesian ABC framework is well-suited for parallel simulations**.
- EIV and EIMAD, both based on the same Bayesian decision theoretic framework but different loss functions, performed similarly and better than the baselines.
- For full details and experiments, see **our full paper**.

RESULTS WITH 2D SYNTHETIC SIMULATION MODELS

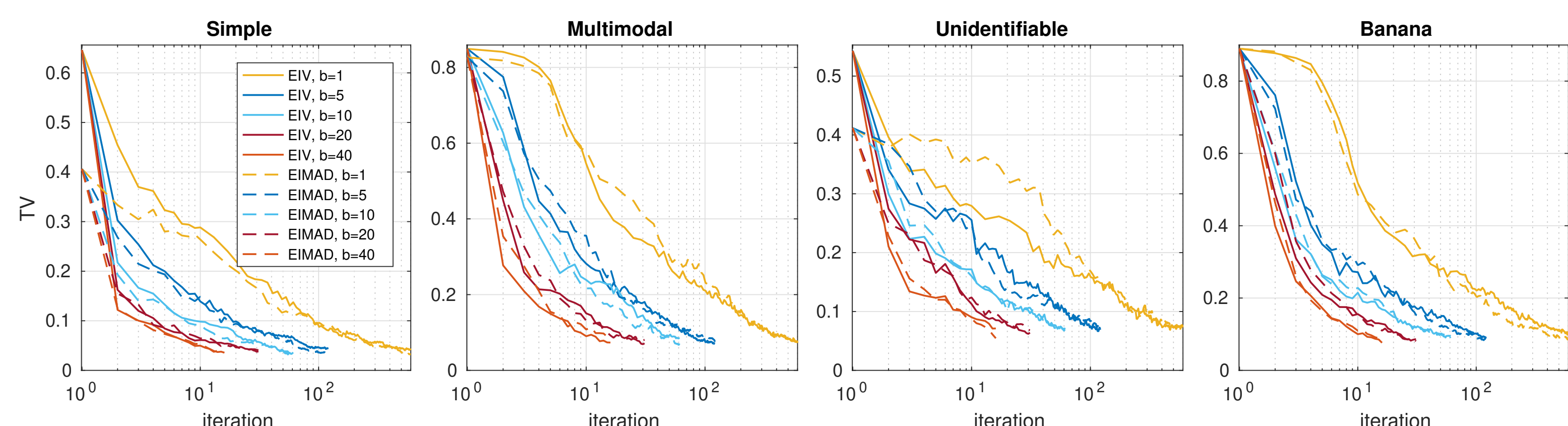


Figure 2: Four 2D toy simulation models using greedy EIV and EIMAD acq. functions and various batch sizes b .

REAL-WORLD TEST CASES: LORENZ AND BACTERIAL INFECTIONS MODELS

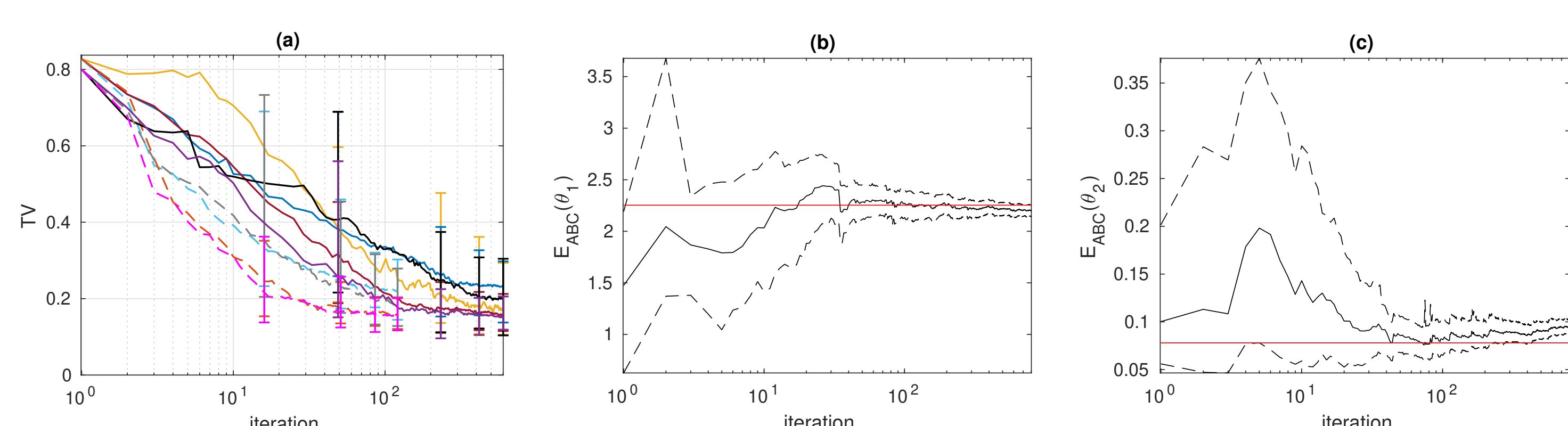


Figure 3: (a) Lorenz model [4, 3]. The intervals show the 90% variability. See Fig. 4a for the legend. (b-c) Black line is the mean and dashed black the 95% CI of the ABC posterior expectations. Red line shows the true value.

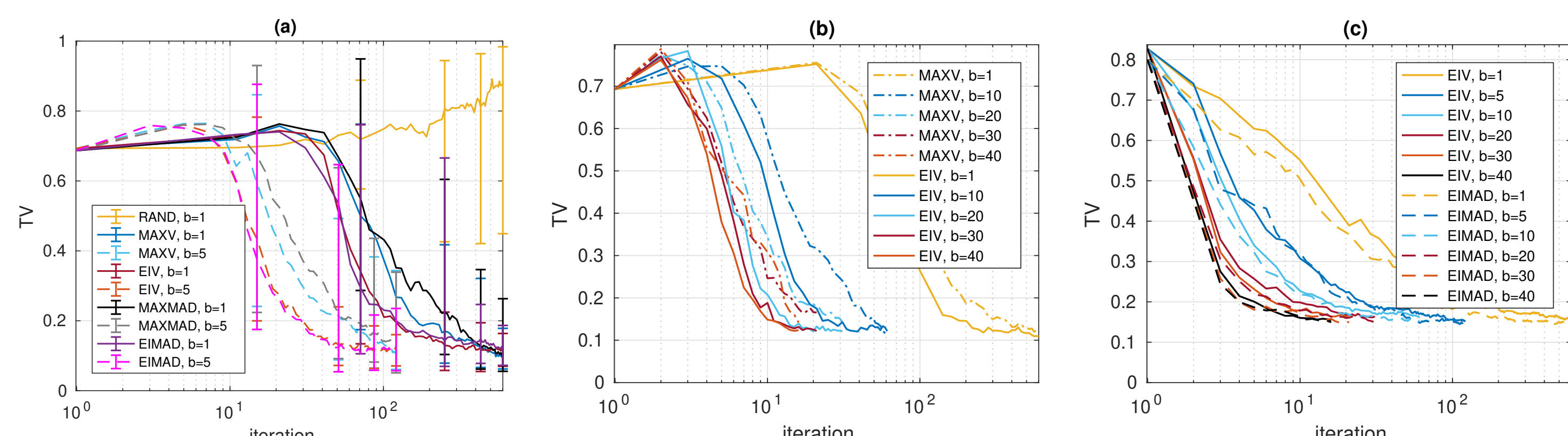


Figure 4: (a) Bacterial infections model [5]. The intervals show the 90% variability. (b) Bacterial infections model with different batch sizes and two chosen acquisition methods. (c) Additional experiments with Lorenz model.

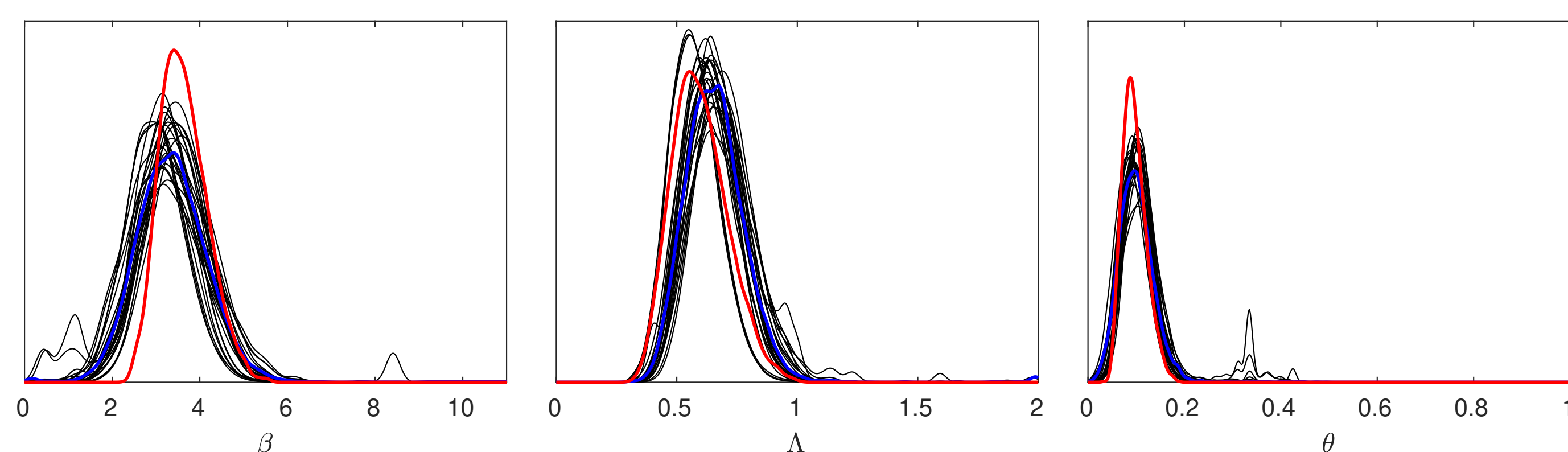


Figure 5: Uncertainty quantification for the ABC posterior marginals of the bacterial infections model after $t = 120$ simulations. Red line: true ABC posterior, blue line: the mean-based point estimate, black lines: sampled ABC marginal posteriors to (approximately) represent the uncertainty due to the limited number of simulations t .